

Accepted Manuscript

Tellurite-exposed *Escherichia coli* exhibits increased intracellular α -ketoglutarate

Claudia A. Reinoso, Christopher Auger, Vasu D. Appanna, Claudio C. Vásquez

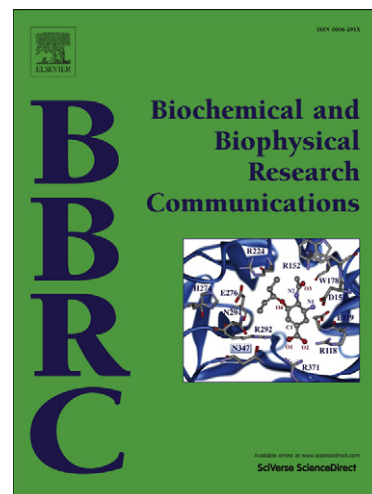
PII: S0006-291X(12)00736-X
DOI: [10.1016/j.bbrc.2012.04.069](https://doi.org/10.1016/j.bbrc.2012.04.069)
Reference: YBBRC 28488

To appear in: *Biochemical and Biophysical Research Communications*

Received Date: 12 April 2012

Please cite this article as: C.A. Reinoso, C. Auger, V.D. Appanna, C.C. Vásquez, Tellurite-exposed *Escherichia coli* exhibits increased intracellular α -ketoglutarate, *Biochemical and Biophysical Research Communications* (2012), doi: [10.1016/j.bbrc.2012.04.069](https://doi.org/10.1016/j.bbrc.2012.04.069)

This is a PDF file of an unedited manuscript that has been accepted for publication. As a service to our customers we are providing this early version of the manuscript. The manuscript will undergo copyediting, typesetting, and review of the resulting proof before it is published in its final form. Please note that during the production process errors may be discovered which could affect the content, and all legal disclaimers that apply to the journal pertain.



1 **Tellurite-exposed *Escherichia coli* exhibits increased intracellular α -**
2 **ketoglutarate**

3

4 Claudia A. Reinoso¹, Christopher Auger², Vasu D. Appanna² and Claudio C.
5 Vásquez^{1*}

6

7

8 ¹Departamento de Biología, Facultad de Química y Biología, Universidad de Santiago de
9 Chile, Santiago, Chile

10

11 ²Department of Chemistry and Biochemistry, Laurentian University, Sudbury, Ontario,
12 Canada

13

14

15

16 ***Corresponding author:** Claudio C. Vásquez, Laboratorio de Microbiología Molecular,
17 Departamento de Biología, Facultad de Química y Biología, Universidad de Santiago
18 de Chile, Casilla 40, Correo 33, Santiago, CHILE. Telephone: (56-2) 718-1117; Fax:
19 (56-2) 681-2108. E-mail: claudio.vasquez@usach.cl

20

21

22 **Abstract**

23

24 The tellurium oxyanion tellurite is toxic to most organisms because of its
25 ability to generate oxidative stress. However, the detailed mechanism(s) how this
26 toxicant interferes with cellular processes have yet to be fully understood. As part
27 of our effort to decipher the molecular interactions of tellurite with living systems,
28 we have evaluated the global metabolism of α -ketoglutarate a known anti-oxidant
29 in *Escherichia coli*. Tellurite-exposed cells displayed reduced activity of the KG
30 dehydrogenase complex (KGDHc), resulting in increased intracellular KG content.
31 This complex's reduced activity seems to be due to decreased transcription in the
32 stressed cells of *sucA*, a gene that encodes the E1 component of KGDHc.
33 Furthermore, it was demonstrated that the increase in total reactive oxygen
34 species and superoxide observed upon tellurite exposure was more evident in wild
35 type cells than in *E. coli* with impaired KGDHc activity. These results indicate that
36 KG may be playing a pivotal role in combating tellurite-mediated oxidative damage.

37

38

39

40

41 **Key words:** tellurite; α -ketoglutarate; superoxide; reactive oxygen species;
42 oxidative stress

43

44

45 Introduction

46

47 Tellurium is a metalloid belonging to the VIA group of the periodic table of
48 elements that shares various chemical properties with biologically important
49 elements such as oxygen, sulfur, and selenium [1]. Although in its elemental form,
50 Te^0 , tellurium is rather scarce in nature, the soluble oxyanions tellurite (TeO_3^{-2}) and
51 tellurate (TeO_4^{-2}) are highly toxic to both prokaryotic and eukaryotic cells [2].
52 Experimental evidence accumulated during the last few years suggests that
53 tellurite toxicity is due, at least in part, to the generation of reactive oxygen species
54 (ROS) [3, 4, 5, 6]. Tellurite-mediated ROS generation was first suggested in
55 studies showing that tellurite minimal inhibitory concentrations (MIC) were higher
56 for tellurite-hypersensitive *Escherichia coli sodAsodB* under anaerobic conditions
57 [7]. The leading ROS generated as consequence of tellurite exposure was shown
58 to be superoxide (O_2^-) [4]. In fact, it was later shown that this radical, produced
59 concomitantly with tellurite reduction, was responsible for the abolition of fumarase
60 and aconitase activity in tellurite-exposed *E. coli* [8].

61 On the other hand, studies using extracts from *Aeromonas caviae* ST and *E.*
62 *coli* previously grown in the presence of increasing K_2TeO_3 concentrations showed
63 that while pyruvate dehydrogenase (PDH) activity decreased by ~40%, tellurite
64 reductase (TR) activity increased almost 2-fold. Only dihydrolipoamide
65 dehydrogenase (E3 component of PDH) was shown to display TR activity *in vitro*
66 [9]. Because E3 also forms part of the α -ketoglutarate dehydrogenase complex
67 (KGDHc) [10] tellurite might also affect the normal functioning of this complex, thus

68 representing another intracellular target of the toxicant [9]. In this context, a
69 perturbation of various key TCA cycle enzymes activity leading to α -ketoglutarate
70 (KG) accumulation has been observed in *Pseudomonas fluorescens* and
71 eukaryotic HepG2 cells exposed to ROS-generating compounds [11].

72 KG, an intermediary α -keto acid of the TCA cycle, can detoxify H_2O_2 and O_2^-
73 through spontaneous decarboxylation to yield succinate [12]. It has been proposed
74 that by decreasing KGDHc and increasing isocitrate dehydrogenase (ICDH)
75 activities, cells seem to dedicate some KG to ROS-scavenging with the
76 concomitant drop in NADH biogenesis. Thus, reducing KGDHc activity seems to be
77 pivotal in TCA cycle regulation [11]. In this context, KGDHc activity modulation
78 could play a key role in the cell's ROS-detoxifying strategy.

79 In this work, we evaluated KG's participation in facing tellurite-induced
80 oxidative stress in *E. coli*. KGDHc activity and KG content was examined in
81 tellurite-exposed *E. coli*. Tellurite sensitivity and ROS content was assessed in wild
82 type and *E. coli* cells lacking *sucA*, *sucB* or *lpdA*, encoding E1 (ketoglutarate
83 dehydrogenase), E2 (dihydrolipoyl transacetylase) and E3 (dihydrolipoyl
84 dehydrogenase) KGDHc components, respectively. Results showed decreased
85 KGDHc activity and increased KG content in toxicant-treated bacteria, suggesting
86 that KG accumulation may represent a strategy to cope with tellurite-mediated
87 oxidative damage in *E. coli*. Reduced KGDHc activity seems to result from
88 decreased *sucA* transcription in stressed cells. Finally, it was observed that *E. coli*
89 exhibiting impaired KGDHc activity generates less ROS than the wild type strain.

90

91 **Materials and Methods**

92

93 Bacteria and growth conditions

94

95 Bacterial strains used in this work are listed in Table 1. Cells were routinely
96 grown in Luria-Bertani (LB) medium at 37 °C with shaking. Growth was started by
97 inoculating 1:100 dilutions of overnight cultures in fresh medium. When required,
98 kanamycin (100 µg/ml) was amended to the medium.

99

100 Growth inhibition zone (GIZ) and minimal inhibitory concentration (MIC)
101 determination

102

103 GIZ were determined as described earlier [13]. In brief, cultures were grown
104 to OD₆₀₀ ~0.5 and 100 µl aliquots were evenly spread on LB-agar plates. After air
105 drying, 10 µl of K₂TeO₃ 10,000 µg/ml were deposited on sterile filter disks (6 mm)
106 previously placed on the plate centers. Growth inhibition zones were determined
107 after overnight incubation at 37 °C.

108 MICs were assessed as follows. Sterile stock solutions of appropriate
109 K₂TeO₃ concentrations were serially diluted in 96-well ELISA plates containing 200
110 µl of LB medium amended with the appropriate antibiotic per well. Cultures (5 µl)
111 grown to OD₆₀₀ ~0.5 were added to each well and plates were incubated at 37 °C.
112 Turbidity was observed visually after 24 h.

113

114 Assessment of intracellular KG and succinate content

115

116 KG levels were determined by high-performance liquid chromatography
117 (HPLC). Cells *E. coli* BW25113 (wild type) were grown in LB medium and exposed
118 to 0.5 µg/ml tellurite for 5, 15 or 30 min. After centrifuging at 8,000 x *g* for 3 min,
119 cells were washed and suspended in 350 µl of 25 mM phosphate buffer pH 7.0.
120 After sonication, the cell debris was discarded and supernatants were treated with
121 200 µl of 0.5% (v/v) perchloric acid and centrifuged and filtered before injection into
122 an Alliance HPLC (Waters) apparatus equipped with an Agilent Hi-Plex H (300 x
123 7.7 mm) column operating at a flow rate of 0.6 ml/min. Runs lasted 30 min. KG and
124 succinate were detected at 210 nm using a dual wavelength absorbance detector.
125 The mobile phase was 5 mM H₂SO₄ at 55 °C. Metabolites were identified by
126 comparison with known standards and bands were quantified using the Empower
127 software (Waters Corporation). Protein concentration was normalized as described
128 earlier [14].

129

130 qRT-PCR

131

132 Cells grown in LB medium to OD₆₀₀ ~0.5 were exposed to 0.5 µg/ml tellurite
133 for 30 min. Total RNA was purified using the RNAsy kit (Qiagen), as
134 recommended. Two µg of purified RNA was used as template for qRT-PCR.
135 Reactions were performed using the LightCycler RNA Amplification SYBR Green I
136 kit (Roche Applied Science) as recommended by the vendor. Transcript amounts

137 (ng) of *sucA*, *sucB* and *lpdA* mRNA were calculated from a standard curve made
138 with known template concentrations. Specific primers used to amplify the genes
139 under study are indicated in Table 1. *rpoD* was used to normalize the experiment.

140

141 ROS monitoring by flow cytometry

142

143 To determine total ROS, *E. coli* BW25113 and KGDHc mutants were grown
144 to OD₆₀₀ ~0.5 and exposed to 0.05 µg/ml tellurite for 30 min. After washing,
145 centrifuging and suspending in 500 µl of 25 mM phosphate buffer pH 7.0 (buffer A),
146 cells were incubated with 0.02 mM 2,7-dihydrodichlorofluorescein diacetate
147 (H₂CFDA, final concentration) for 30 min in the dark. Fluorescence intensity was
148 monitored as above (λ_{ex} 428, λ_{em} 522). Data acquisition was performed by counting
149 the number of positive cells as recently described [15]. Cells exposed to 5 mM TBH
150 (tert-butyl hydroperoxide) were used as positive control for total ROS detection.

151 To assess superoxide, *E. coli* BW25113 and KGDHc mutants strains were
152 grown to OD₆₀₀ ~0.5 and exposed to 0.05 µg/ml tellurite for 30 min. After
153 centrifuging and washing with buffer A, cells were suspended in 500 µl of buffer A
154 and incubated with 0.05 mM dihydroethidine (DHE, final concentration) for 15 min
155 in the dark. Intensity was assessed using a Becton Dickinson (model FacsCanto II)
156 apparatus equipped with an Argon laser (λ_{ex} 520, λ_{em} 610). Tellurite-exposed
157 $\Delta\text{sodAsodB}$ *E. coli* was used as tool for oxidized DHE detection.

158

159

160 KGDHc, complex I and NADH oxidase activity determination

161

162 KGDHc activity was assayed at 37 °C in cell-free extracts from tellurite-
163 exposed *E. coli* (0.5 µg/ml, 30 min). NAD⁺ reduction was monitored at 340 nm for 1
164 min. The reaction mixture (1 ml) contained 25 mM Tris-HCl buffer, pH 7.0, 0.5 mM
165 NAD⁺, 10 mM KG, 20 mM MgSO₄, 1 mM CoASH and 4 mM TPP. Assays were
166 started with the extract (100 µg protein) [16]. Blue native polyacrylamide gels were
167 run for in-gel visualization of enzyme activity. Assays were started with the extract
168 (300 µg protein) coupling NADH/NADPH formation to 0.3 mg/ml phenazine
169 methosulfate and 0.5 mg/ml idonitrotetrazolium as decribed [17].

170 Complex I and NADH oxidase activity was assessed at 37 °C in cell-free
171 extracts from tellurite-exposed *E. coli* (0.5 µg/ml, 30 min). Blue native
172 polyacrylamide gels were run for in-gel visualization of enzyme activity and then
173 incubated with 25 mM Tris-HCl pH 7.4, 5 mM MgCl₂ buffer for 15 min. Assays were
174 started with the extract (100 µg protein), after adding 5 mM NADH and 5 mM KCN,
175 0.4 mg/ml idonitrotetrazolium and 0.2 mg/ml dichlorophenol indophenol were
176 used to reveal the activity [17].

177

178 Data analysis

179 In general, results were expressed as the mean ± the standard deviation.

180 Differences between experimental groups were analyzed using one-way ANOVA.

181 P values less than 0.05 were considered statistically significant.

182 Results and Discussion

183

184 *E. coli* exposure to tellurite results in decreased KGDHc activity and unchanged
185 complex I and NADH oxidase activities

186

187 To assess the effect of tellurite on KGDHc activity, extracts from tellurite-
188 exposed cells were used. As determined by a spectrophotometric assay,
189 enzymatic activity decreased ~30% when wild type *E. coli* was exposed to the
190 toxicant for 30 min (Fig. S1A). KGDHc activity was also assessed *in situ*, after
191 fractionating crude extracts from cells exposed or not to tellurite by non-denaturing
192 polyacrylamide gel electrophoresis. KGDHc activity was practically undetected
193 even after 24 h exposure (Fig. 1A). KGDHc activity abolition could be the
194 consequence of a direct effect of tellurite on enzyme activity/structure or indirect, at
195 the transcriptional level thus affecting mRNA synthesis for one (or more) KGDH
196 components (see below).

197 On the other hand, it has been proposed that KG decarboxylation -with the
198 concomitant NADH formation- would increase the oxidative status of the cell [18].
199 KGDHc inhibition/inactivation would help to alleviate the effects of tellurite-
200 mediated oxidative damage. In this context, there are other examples regarding the
201 role that metabolic enzymes could play in controlling oxidative damage caused by
202 certain elicitors as aluminium [19] or tellurite [8, 9].

203 Given that limiting NADH production is crucial under oxidative stress
204 conditions and since the activity of NADH-using enzymes usually decreases in

205 these circumstances [20], the activity of complex I and NADH oxidase was
206 assessed. No significant changes in these activities were observed in tellurite-
207 exposed cells when compared with untreated controls (Fig. 1B), evidencing the
208 importance of decreasing NADH levels through KGDHc inhibition to alleviate
209 tellurite-mediated oxidative stress.

210

211 KG accumulates in tellurite-exposed *E. coli* cells

212

213 Since KGDHc activity decreases in tellurite-exposed *E. coli*, KG content was
214 assessed by high performance liquid chromatography (HPLC). Higher KG levels
215 were found in tellurite-exposed wild type cells in regard to untreated controls (Fig.
216 2A). These results suggest that KG may accumulate because of the decrease of
217 KGDHc activity. Results supporting this came from the observation that decreased
218 ICDH and GDH KG-synthesizing activities were found in toxicant-exposed *E. coli*
219 (unpublished observations). All of these findings could help the bacterium in facing
220 oxidative stress.

221 Conversely to KG, succinate content decreased in tellurite-treated cells (Fig.
222 2B). Since KG decarboxylation occurs non enzymatically in the presence of H₂O₂
223 or superoxide to yield succinate and CO₂ [12], one would expect to some extent
224 that the increased KG content observed in tellurite-exposed cells results in
225 augmented succinate levels. Probably succinate amounts could be augmented
226 only after enough KG is accumulated and thus succinate coming from KG

227 decarboxylation would serve to keep the Krebs cycle at work under basal
228 conditions.

229

230 Transcriptional level of *sucA*, *sucB* and *lpdA* in tellurite-exposed *E. coli*

231

232 To assess if the observed decrease of KGDHc activity in tellurite-treated
233 cells was related to the amount of *sucA*, *sucB* or *lpdA* transcripts, their levels were
234 analyzed by qPCR. Significant changes were observed only for the *sucA* gene.
235 While *sucB* and *lpdA* transcription was not altered significantly, that of *sucA* was
236 decreased by ~50% (Fig. S1B). Although not totally conclusive, these results
237 possibly reveal that tellurite inhibits KGDHc activity by affecting the amount of the
238 E1 component transcript rather than exerting a direct effect on the [(SucA)₁₂-
239 (SucB)₂₄-(Lpd)₂] multienzyme complex. Decreased *sucA* transcription would result
240 in less SucA to form further complexes and hence in decreased enzymatic activity,
241 which also would slow the functioning of the Krebs cycle. Decreased *E. coli sucA*
242 transcription has also been observed in *E. coli* cells exposed to TiO₂ [21].

243

244 Tellurite susceptibility of *E. coli* deficient in KG metabolism

245

246 A wild type *E. coli* as well as Δ *sucA*, Δ *sucB* and Δ *lpdA* strains was analyzed
247 to assess tellurite tolerance. All mutant derivatives showed increased tellurite
248 sensitivity in regard to the isogenic, parental strain (Table 2). Particularly
249 interesting was the Δ *lpdA* strain, which was eight-fold more sensitive to tellurite

250 than wild type cells. It should be noted that tellurite concentrations used in these
251 experiments could affect, in addition to the Krebs cycle, other metabolic pathways
252 such as glycolysis [22], the pentose phosphate shunt and/or the electron transport
253 chain (unpublished data), which would inhibit bacterial growth.

254

255 ROS content in tellurite-exposed *E. coli*

256

257 Total ROS as well as superoxide content was assessed in tellurite-exposed
258 *E. coli*. Regarding the respective untreated controls, increased levels of superoxide
259 and total ROS were observed in all tellurite-treated cells (Figs. 3 and 4). Increased
260 levels of these species were more evident in the wild type strain. At least 20% less
261 total ROS was observed in tellurite-treated mutant strains as compared to the wild
262 type counterpart. This could be interpreted as the lack of KGDHc activity in mutant
263 strains resulting in KG accumulation which could be used in ROS scavenging.

264 Finally, all tested strains exhibited high basal superoxide levels. This could
265 be explained because KGDHc inhibition/inactivation would interrupt the functioning
266 of the Krebs cycle, which in turn would result in a decreased cellular antioxidant
267 pool. In addition, dihydroethidine becomes very toxic after being oxidized by
268 superoxide because of its interaction with DNA [23]. Regarding the respective
269 controls, fluorescence intensity increased 37, 28, 7 and 28% in tellurite-exposed
270 wild type, $\Delta sucA$, $\Delta sucB$ and $\Delta lpdA$, respectively. These results support those
271 obtained when analyzing total ROS content. To shed further light to the tellurite

272 effect on global KG metabolism, experiments regarding KG biosynthesis upon
273 tellurite exposure are currently being carried out in our laboratory.

274

275 **Acknowledgements**

276

277 This work was supported in part by grants # 1090097 from Fondecyt (Fondo
278 Nacional de Investigación Científica y Tecnológica) and Dicyt-USACH (Dirección
279 de Investigación en Ciencia y Tecnología-Universidad de Santiago de Chile) to
280 C.C.V. C.A.R. was supported by a doctoral fellowship CONICYT (Comisión
281 Nacional de Investigación Científica y Tecnológica). C.A. was supported by the
282 Ontario Graduate Scholarship and Laurentian University.

283

284 **References**

285

286 [1] D. Taylor, Bacterial tellurite resistance, Trends Microbiol. 7(1999)111-115.

287

288 [2] S. Baesman, T. Bullen, J. Dewald et al., Formation of tellurium nanocrystals
289 during anaerobic growth of bacteria that use Te oxyanions as respiratory electron
290 acceptors, Appl. Environ. Microbiol. 73 (2007) 2135-2143.

291

292 [3] F. Borsetti, V. Tremaroli, F. Michelacci et al., Tellurite effects on *Rhodobacter*
293 *capsulatus* cell viability and superoxide dismutase activity under oxidative stress
294 conditions, Res. Microbiol. 156 (2005) 807-813.

295 [4] I. Calderón, F. Arenas, J.M Pérez et al., Catalases are NAD(P)H dependent
296 tellurite reductases, PLoS ONE 1(2006) e70.

297

298 [5] V. Tremaroli, F. Fedi, D. Zannoni, Evidence for a tellurite-dependent generation
299 of reactive oxygen species and absence of a tellurite-mediated adaptive response
300 to oxidative stress in cells of *Pseudomonas pseudoalcaligenes* KF707, Arch.
301 Microbiol. 187(2006)127-135.

302

303 [6] J.M. Pérez, I.L. Calderón, F.A. Arenas et al., Bacterial toxicity of potassium
304 tellurite: unveiling an ancient enigma, PLoS ONE 2 (2007) e211.

305

306 [7] J. Tantaleán, M. Araya, S. Pichuantes et al., The *Geobacillus*
307 *stearothermophilus* V *iscS* gene, encoding cysteine desulfurase, confers resistance
308 to potassium tellurite in *Escherichia coli* K-12, J. Bacteriol. 185 (2003) 5831-5837.

309

310 [8] I.L. Calderón, A.O. Elías, E.L. Fuentes et al., Tellurite-mediated disabling of
311 4Fe-4S clusters of *Escherichia coli* dehydratases, Microbiology 155 (2009)1840-
312 1846.

313

314 [9] M.E. Castro, R. Molina, W. Díaz et al., The dihydrolipoamide dehydrogenase of
315 *Aeromonas caviae* ST exhibits NADH-dependent tellurite reductase activity,
316 Biochem. Biophys. Res. Commun. 375 (2008) 91-94.

317

318 [10] A. De Kok, A.F. Hengeveld, A. Martin et al., The pyruvate dehydrogenase
319 multi-enzyme complex from Gram-negative bacteria, *Biochim. Biophys. Acta* 1385
320 (1998) 353-366.

321

322 [11] R.J Mailloux, R. Bériault, J. Lemire et al., The tricarboxylic acid cycle, an
323 ancient metabolic network with a novel twist, *PLoS ONE* 2 (2007) e690.

324

325 [12] N.I. Fedotcheva, A.P. Sokolov, M.N. Kondrasshova, Nonenzymatic formation
326 of succinate in mitochondria under oxidative stress, *Free Radic. Biol. Med.*
327 41(2006) 56-64.

328

329 [13] D.E. Fuentes, E.L. Fuentes, M.E. Castro et al., Cysteine metabolism-related
330 genes and bacterial resistance to potassium tellurite, *J. Bacteriol.* 189 (2007) 8953-
331 8960.

332

333 [14] M. Bradford, A rapid and sensitive method for quantitation of microgram
334 quantities of protein utilizing the principle of protein-dye-binding, *Anal. Biochem.* 72
335 (1967) 248-254.

336

337 [15] G.A. Pradenas, B.A. Paillavil, S. Reyes-Cerpa et al., Reduction of the
338 monounsaturated fatty acid content of *Escherichia coli* K-12 results in increased
339 resistance to oxidative damage, *Microbiology* 158 (2012) 1279-1283.

340

341 [16] R. Hamel, V. Appanna, Modulation of TCA cycle enzymes and aluminum
342 stress in *Pseudomonas fluorescens*, J Inorg Biochem. 87(2001) 1-8.

343

344 [17] R. Singh, D. Chénier, R. Bériault et al., Blue native polyacrylamide gel
345 electrophoresis and the monitoring of malate- and oxaloacetate-producing
346 enzymes, J. Biochem. Biophys. Methods 64 (2005) 189-199.

347

348 [18] R. Mailloux, R. Singh, G. Brewer et al., α -ketoglutarate dehydrogenase and
349 glutamate dehydrogenase work in tandem to modulate the anti-oxidant α -
350 ketoglutarate during oxidative stress in *Pseudomonas fluorescens*, J. Bacteriol.
351 191(2009) 3804-3810.

352

353 [19] J. Middaugh, R. Hamel, G. Jean-Baptiste et al., Aluminum triggers decreased
354 aconitase activity via Fe-S cluster disruption and the overexpression of isocitrate
355 dehydrogenase and isocitrate lyase: a metabolic network mediating cellular
356 survival, J. Biol. Chem. 280 (2005) 3159-3165.

357

358 [20] R. Singh, R. Mailloux, S. Puisseux-Dao, V.D. Appanna, Oxidative stress evokes
359 a metabolic adaptation that favors increased NADPH synthesis and decreased
360 NADH production in *Pseudomonas fluorescens*, J. Bacteriol. 189 (2007) 6665-
361 6675.

362

363 [21] Y. Ojima, M. Nishioka, M. Taya, Metabolic alternations in SOD-deficient
364 *Escherichia coli* cells when cultivated under oxidative stress from photoexcited
365 titanium dioxide, *Biotechnol. Lett.* 30 (2008) 1107-1113.

366

367 [22] M.A. Valdivia, J.M. Pérez-Donoso, C.C. Vásquez, Effect of tellurite-mediated
368 oxidative stress on the *Escherichia coli* glycolytic pathway, *Biometals* 25 (2012)
369 451-458.

370

371 [23] C.D. Georgiou, I. Papapostolou, N. Patsoukis, T. Tsegenidis, T. Sideris, An
372 ultrasensitive fluorescent assay for the in vivo quantification of superoxide radical
373 in organisms, *Anal. Biochem.* 347 (2005) 144-151.

374

375

376

377

378

379

380

381

382

383

384

385

386 **Figure legends**

387

388 **Fig. 1.** *In situ* KGDHc, complex I and NADH oxidase activity. KGDHc (A) and
389 complex I and NADH oxidase activities (B) were assayed after fractionating
390 extracts from tellurite-treated cells by native gradient polyacrylamide gels as
391 described in Methods. Representative gels are shown.

392

393 **Fig. 2.** Metabolite assessment in tellurite-exposed wild type *E. coli*. KG (A) and
394 succinate (B) contents in wild type *E. coli* exposed to 0.5 µg/ml tellurite for 5, 15
395 and 30 min. were assessed by HPLC as described in Methods. The line represent
396 negative control for both compounds (no tellurite added). Numbers represent the
397 mean of 3 independent trials. ns, non significant.

398

399 **Fig. 3.** Total ROS levels in tellurite-exposed *E. coli*. The indicated *E. coli* strains
400 exposed or not to tellurite or tert-butyl hydroperoxide (TBH) were assessed for total
401 ROS content by flow cytometry using 2',7'-dihydrodichlorofluorescein diacetate as
402 described in Methods. Dot Plot representation, X axis represents fluorescence
403 intensity and Y axis forward scattering (FCS). A, wild type; B, $\Delta sucA$; C, $\Delta sucB$; D,
404 ΔpdA .

405

406

407

408

409 **Fig. 4.** Superoxide generation in tellurite-exposed *E. coli*. The indicated *E. coli*
410 strains exposed or not to tellurite were assessed for superoxide content by flow
411 cytometry using dihydroethidine as described in Methods. Dot Plot representation,
412 X axis represents fluorescence intensity and Y axis forward scattering (FCS). A,
413 wild type; B, $\Delta sodAB$; C, $\Delta sucA$; D, $\Delta sucB$; E, $\Delta lpdA$.

414

415 **Fig. S1.** KGDHc activity and transcriptional level of KGDH-encoding genes in
416 tellurite-exposed *E. coli*. A, spectrophotometric determination of KGDHc activity in
417 extracts of wild type cells; B, Transcriptional level of KGDH-encoding genes in
418 tellurite-exposed *E. coli*. Values above or below the line indicate increased or
419 decreased transcription, respectively. Numbers represent the mean of 3
420 independent trials.

421

422

423

424

425

426

427

428

429

430

431

432

433

434

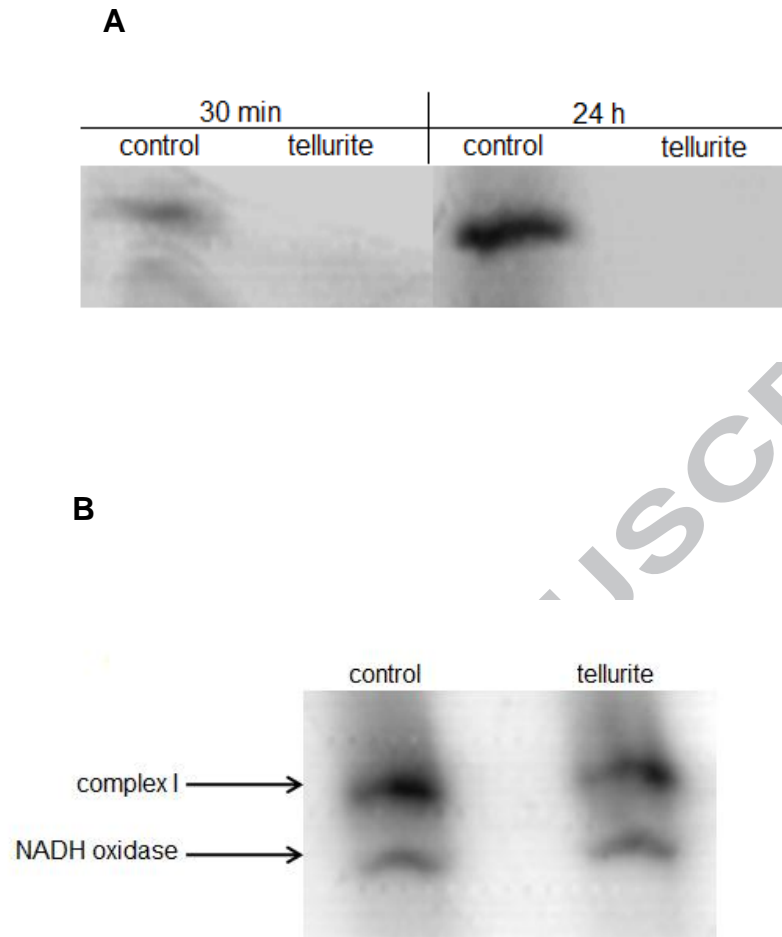
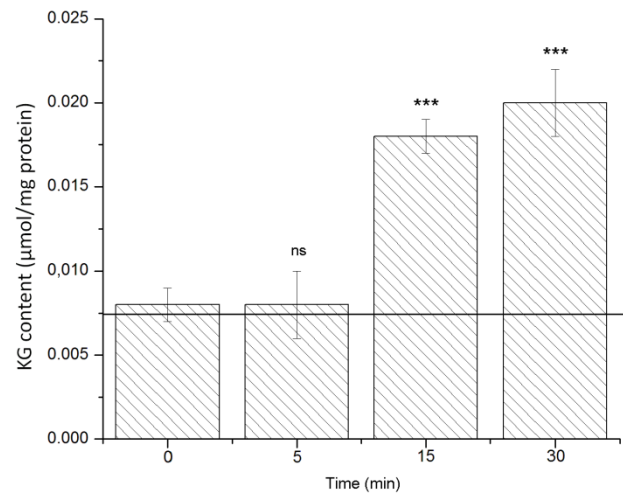
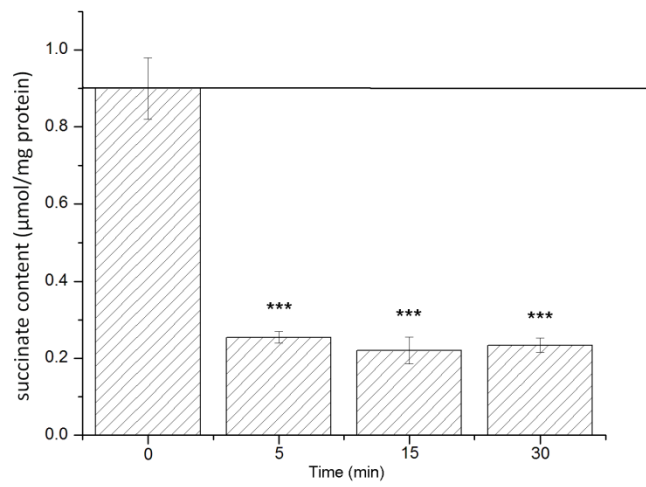


Fig. 1. Reinoso *et al.*

ACCEPTED MANUSCRIPT

A**B****Fig. 2.** Reinoso *et al.*

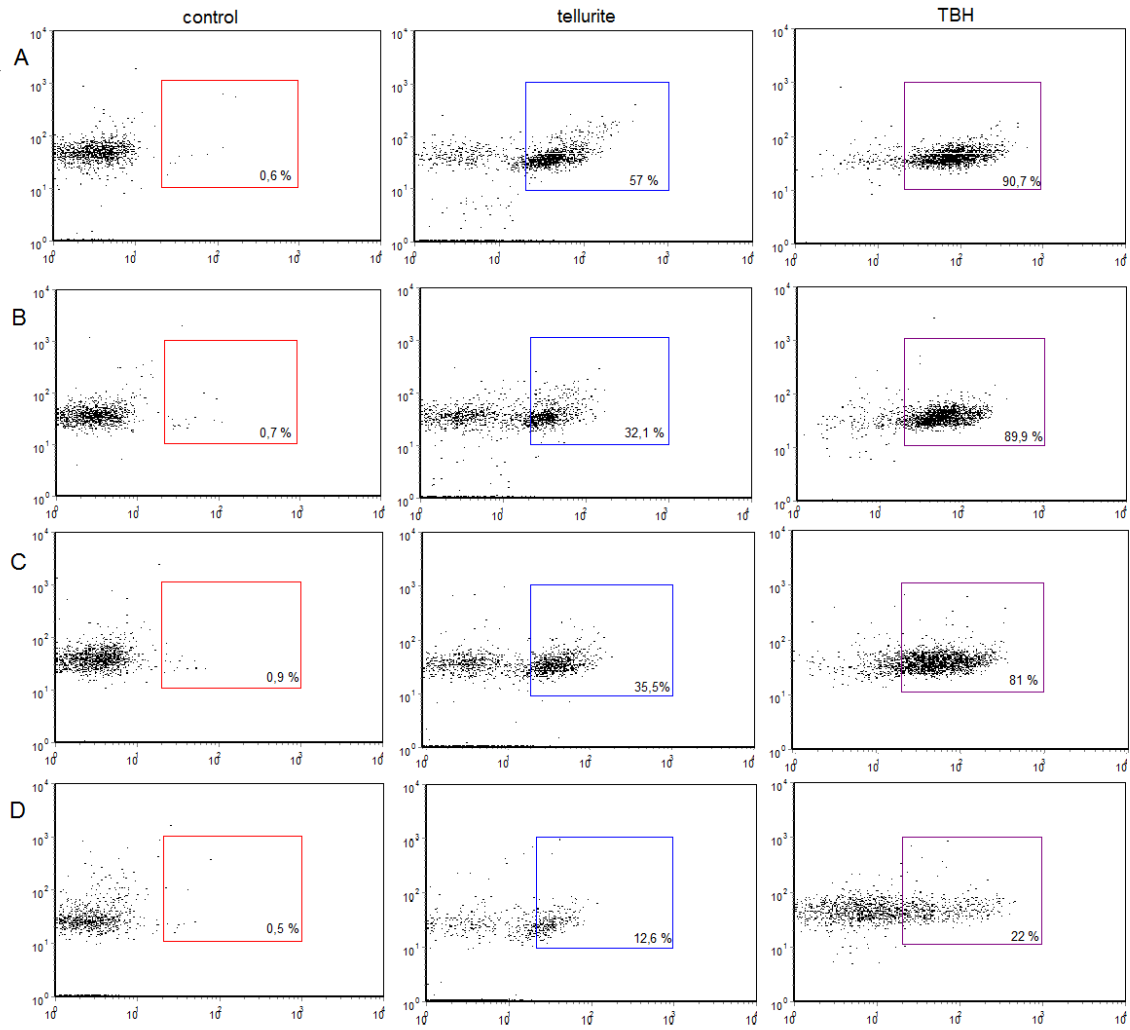


Fig. 3. Reinoso *et al.*

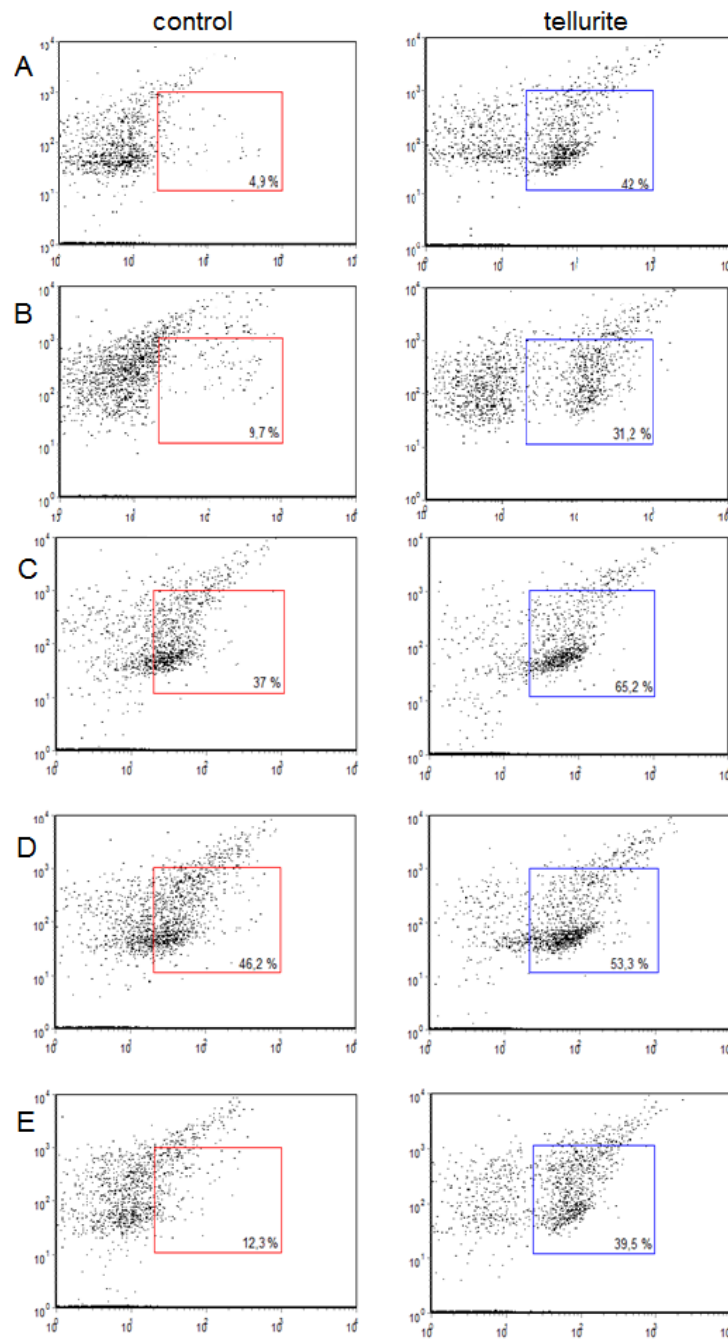


Fig. 4. Reinoso *et al.*

Table 1. *E. coli* strains and primers used in this study

Strain	Relevant genotype	Source or reference
BW25113	$\Delta(\text{araD-araB})567, \Delta(\text{lacZ4787}>::\text{rrnB-3}),$	Baba et al. 2006
ΔsucA	BW25113 <i>sucA</i> (<i>icdA</i> ::Kan ^R)	Baba et al. 2006
ΔsucB	BW25113 <i>sucB</i> (<i>sucB</i> ::Kan ^R)	Baba et al. 2006
ΔlpdA	BW25113 <i>lpdA</i> (<i>lpdA</i> ::Kan ^R)	Baba et al. 2006

Primers	Forward (F) or Reverse (R), to amplify	5'-3' Sequence
<i>sucA</i> F	F, <i>sucA</i>	ATGCAGAACAGCGCTTTGAA
<i>sucA</i> R	R, <i>sucA</i>	CGGAAATATTCACGCGTTTG
<i>sucB</i> F	F, <i>sucB</i>	CTGACCTGCCTGAATCCGTA
<i>sucB</i> R	R, <i>sucB</i>	ACCAAGGATCTGACGAGACG
<i>lpdA</i> F	F, <i>lpdA</i>	GTAAGTAAATCAAACTCAGGTCTG
<i>lpdA</i> R	R, <i>lpdA</i>	CGCTTTGGCTTCTTCGATAA

Table 2. Tellurite GIZ (cm²) and MIC (μg/ml) for the indicated *E. coli* strains

Strains	GIZ	MIC
BW25113	7.1	0.8
<i>ΔsucA</i>	7.4	0.4
<i>ΔsucB</i>	7.8	0.4
<i>ΔlpdA</i>	9.9	0.1

GIZs and MICs were determined in LB medium as described in Methods. Numbers are the mean of 3 independent trials.

- 1.- Tellurite-exposed *E. coli* exhibits decreased α -KG dehydrogenase activity
- 2.- Cells lacking α -KGDH genes are more sensitive to ROS than isogenic, wt *E. coli*
- 3.- KG accumulation may serve to face tellurite-mediated oxidative damage in *E. coli*

ACCEPTED MANUSCRIPT